Feasibility of Tumor Imaging Using L-3-[Iodine-123]-Iodo-α-Methyl-Tyrosine in Extracranial Tumors

Pieter L. Jager, Eric J.F. Franssen, Walter Kool, Ben G. Szabó, Harald J. Hoekstra, Harry J.M. Groen, Elizabeth G.E. de Vries, Gustaaf W. van Imhoff, Willem Vaalburg and D. Albertus Piers

Departments of Nuclear Medicine, Radiotherapy, Surgical Oncology, Pulmonology, Medical Oncology, Hematology and PET Center, University Hospital Groningen, Groningen, The Netherlands

L-3-[^{123}I]-Iodo-α-methyl-tyrosine (IMT) is a modified amino acid. It is reported to be avidly taken up in brain tumors, reflecting amino acid transport and is suitable for SPECT. **Methods:** To determine whether tumors outside the brain can also accumulate this tracer, we injected 300–450 MBq IMT into 20 patients with different tumors [5 breast cancers, 4 lung tumors (1 benign), 2 carcinoid liver metastases, 4 soft-tissue tumors (1 benign), 3 malignant lymphomas and 2 primary brain tumors]. Tumor size ranged from 1–12 cm. Imaging was repeated after radiotherapy in two patients with breast cancer. Histology was available in all cases. Dynamic scans, whole-body imaging and SPECT were performed during the first hour and 3 hr after injection. Plasma samples were analyzed for IMT, free ^{123}I and other metabolites. **Results:** All primary tumors were visualized. Tumor-to-background ratios ranged from 1.1 to 3.8 on planar and from 1.3 to 6.2 on SPECT images. Tumor uptake peaked in the first hour. Two carcinoid lesions in the liver tumors exhibited no IMT uptake above liver background. Tumor-to-background ratios in a benign bone inflammatory process and a focal pulmonary vasculitis were less than 1.2 (planar) and 1.9 (SPECT) and could be differentiated from uptake in all malignant nonbrain tumors. IMT was rapidly cleared from the plasma [3.6% ± 0.6% (mean ± s.d.) injected dose/liter at 10 min postinjection]. Minor in vivo deiodination was present (<1% of injected dose 1 hr postinjection). No other metabolites were found. Normal distribution consists of some uptake in the brain, liver, spleen, muscles, pancreatic region and intestinal structures and massive uptake and excretion in the kidneys and bladder. **Conclusion:** IMT has potential as a metabolic tracer in tumors outside the brain.

Key Words: tumor imaging; amino acids; iodine-123-methyl-tyrosine; SPECT

J Nucl Med 1998; 39:1736–1743

Considerable interest has been shown in metabolic imaging of tumors using PET with ^{18}F-fluorodeoxyglucose (FDG) or radiolabeled amino acids such as L-[^{11}C-methyl]-methionine or L-[1-^{11}C]-tyrosine (*1–3*). Uptake of these tracers in tumors is based on the increased metabolic demand of tumor tissue compared with normal tissue and is hypothesized to represent tumor vitality (*4–6*). These tracers have several potential uses in oncology, including characterization of anatomic lesions, tumor staging and evaluation of therapy. Fluorine-18-FDG is taken avidly up by almost all kinds of tumors, representing increased glucose consumption, but it also accumulates in inflammatory tissues (*7,8*). Several studies have suggested that imaging with radiolabeled amino acids visualizes protein synthesis and amino acid transport phenomena (*9–11*). These processes are generally accelerated in tumors (*12*). Because amino acids play a minor role in the metabolism of inflammatory cells, these tracers might be more tumor specific than FDG (*13,14*)

Because of the limited availability and cost of PET, there is a demand for similar compounds for use in a conventional nuclear medicine department. SPECT using FDG is an option, but aside from the limited specificity, clinical oncologic application is hampered by detection difficulties such as a limited resolution, low sensitivity for small lesions and septal penetration in ultra-high-energy collimators (*15*).

The ^{123}I-labeled amino acid L-3-[^{123}I]-iodo-α-methyl-tyrosine (IMT) has been introduced for imaging of brain tumors. It was demonstrated that uptake in brain tumors represents amino acid transport and, thus, a step in tumor metabolism (*16–20*). IMT is not incorporated into protein. Increased transmembrane transport is thought to be the main determinant of the uptake process (*16*). Sensitivity and specificity are both reported to be between 80% and 100% (*18,19,21*). Interestingly, the uptake increases with higher grading of gliomas, and differentiation between high- and low-grade gliomas appears to be feasible (*21*). IMT uptake changes may predict the response to chemo- and radiotherapy and detect recurrent brain tumors (*22–24*).

IMT was applied as a melanoma-seeking agent and used for scintigraphy of the adrenals and pancreas, both mainly in animal studies, some 20 yr ago (*25,26*). In experimental rat tumors, IMT uptake was found to be associated with amino acid transport, tumor perfusion and diffusion (*27*). Because of the good uptake of ^{11}C-tyrosine demonstrated with PET in various tumors outside the brain (*28–30*) and the initial common step (amino acid transport from plasma into the cell) in the proposed uptake mechanism, we undertook a study to determine whether IMT is taken up in human tumors outside the brain and, if so, to what extent and at what time. In addition, normal uptake patterns were qualitatively studied.

MATERIALS AND METHODS

Patients

Twenty patients (10 male, 10 female; age range 23–81 yr; mean age 61 yr), with known or suspected malignancies, were recruited randomly from various clinical oncologic departments. For all patients, histopathologic material was obtained by biopsy or operation after the IMT study. The selection criterion was the availability of a histologic diagnosis and a location outside the vicinity of the kidneys and the urinary tract (because IMT is excreted by the kidneys). All patients were studied 1–3 wk before therapy was started. Eighteen of the 20 patients had a malignant tumor; in 2 cases, benign inflammatory processes were confirmed by histology. Two patients with breast cancer were studied twice,

Received Aug. 5, 1997; revision accepted Jan. 20, 1998.

For correspondence or reprints contact: P.L. Jager, MD, Department of Nuclear Medicine, University Hospital Groningen, P.O. Box 30001, 9700 RB Groningen, The Netherlands.

TABLE 1
Patient Characteristics and L-3-Iodine-123-Iodo-α-Methyl-Tyrosine Uptake Results

Patient no.	Age (yr)	Sex	Tumor histology	Size (cm)	Visual score*		Tumor-to-background (T/B) ratio*		Remarks
					Planar	SPECT†	Planar	SPECT†	
1	70	F	Carcinoid liver metastasis	1	—		—		Small lesion, no SPECT
2	73	M	Carcinoid liver metastasis	5	—		—		No SPECT
3	76	M	Lung cancer (non-small cell)	4	+	++	1.4	2.5	No other lesions present
4	72	F	Lung cancer (non-small cell)	4	+	++	2.0	3.8	Mediastinal involvement (CT) detected
5	52	M	Lung cancer (small cell)	3	++	+++	1.8	3.0	All metastases (mediastinum, supraclavicular) detected
6	62	M	Lung vascilitis lesion (benign)	2	—	+	1.1	1.7	Benign very active inflammatory process
7	76	F	Breast cancer (ductal)	4	++	+++	2.6	6.2	Axillary lesion 3 cm detected with T/B ratio = 6.2
7A			7: After radiotherapy	0	+	+	1.2	2.3	
8	54	F	Breast cancer (ductal)	4	++		3.6		Two small bone metastases (bone scan) not detected
8A			8: After radiotherapy	1	+	+	1.6	2.1	
9	57	F	Breast cancer (ductal)	3	+	++	1.6	4.0	Axillary micrometastasis not detected
10	81	F	Breast cancer (ductal)	3	+	++	1.3	2.1	One possible bone metastasis not detected
11	45	F	Breast cancer (ductal)	3	+	+++	2.3	4.8	No other lesions
12	82	M	Malignant fibrous histiocytoma (leg)	8	+++		3.0		No other lesions present
13	57	F	Bone tumor, femur (benign)	12	—	+	1.1	1.9	MRI: osteoblastoma: biopsy: benign, inflammation
14	29	M	Mesenchymal chondrosarcoma (elbow)	2	+		1.7		Axillary micrometastasis not detected
15	66	M	High-grade sarcoma (knee)	8	++	+++	3.8	4.8	No other lesions
16	23	M	Mixed oligoastrocytoma	5	—	+	—	1.3	Low-grade process
17	76	F	Glioblastoma multiforme	3	—	+	—	1.2	
18	69	M	Non-Hodgkin's lymphoma (arm)	5	++		1.5		T-cell lymphoma of the skin
19	48	M	Hodgkin's lymphoma (chest)	4	++	+++	1.5	2.4	No other lesions
20	55	F	Hodgkin's lymphoma (chest)	5	++	+++	1.8	2.8	No other lesions

*— = not visible; + = just visible; ++ = visible; +++ = clearly visible.
†Blanks indicate that no SPECT was performed.
Planar was performed 20 min postinjection; SPECT was performed 60 min postinjection.

both before and 6 wk after the termination of external radiotherapy. Table 1 summarizes patient characteristics.

Written informed consent was obtained from all patients. The study was approved by the Medical Ethics Committee of the Groningen University Hospital.

Synthesis and Quality Control

Synthesis of IMT was performed as described by Krummeich et al. (*31*). Briefly, Iodo-gen iodination with high-quality $Na^{123}I$ (specific activity, >5000 Ci/mmol, obtained from Amersham Cygne, Eindhoven, the Netherlands) of the precursor L-α-methyl-tyrosine was performed in a borate buffer. IMT was purified by elution with physiologic saline containing 5% ethanol over a C-18 SepPak cartridge (Waters, Milford, MA) preconditioned with methanol followed by physiologic saline containing 5% ethanol. After filtration through a sterile 0.22-μm Millex GV filter (Millipore, Molsheim, France), a colorless, ready-to-inject solution was obtained. Samples were demonstrated to be sterile and pyrogen-free. Quality control was performed by high-performance liquid chromatography on a RP-18 column (Multosorb 100 4.6) using H_2O/ethanol/acetic acid (87.5:10:2.5, v/v/v), containing 2.5 g/liter ammoniumacetate as eluent. Radiochemical purity was over 99% in all cases. The overall synthesis time, including purification and quality control, was less than 1 hr. Radiochemical yield was 50%–65%.

Imaging

After an overnight fast, imaging was started immediately after the intravenous injection of 300–450 MBq IMT. Fifteen minutes before injection, 10 drops of Lugol's solution were given orally to prevent possible thyroid uptake of free ^{123}I. A large-field-of-view double-head gamma camera (MULTISPECT 2; Siemens Inc., Hoffman Estates, IL) was used with a medium-energy, all-purpose collimator and a 15% window centered on the 159-keV photopeak of ^{123}I. System resolution was 12 mm FWHM at 10 cm distance.

A 30-min dynamic scan (60 frames of 30 sec each) of the tumor

area was acquired in a 128 × 128 matrix, followed by whole-body scanning or SPECT of the tumor area. After SPECT, additional spot views were recorded to obtain whole-body information in all cases. SPECT included 64 views (2 × 32; 5.6°/step) of 40 sec each in a 128 × 128 matrix format with a zoom factor of 1.45. This corresponds to a pixel dimension of 3.3 mm. Whole-body scans were performed with a scan speed of 15 cm/min. The initial scan procedures took 60–80 min. After these initial scans, patients were allowed to eat. SPECT with additional spot views or total body scanning was repeated 3 hr postinjection and also at 24 hr postinjection in the first three patients.

Transaxial tomograms were reconstructed, without prefiltering, using filtered backprojection with a Butterworth filter of sixth order and a cutoff frequency of 0.275 Nyquist. No attenuation correction was performed, except for brain SPECT studies, in which first-order correction using Chang's method was applied with an attenuation coefficient of 0.11 cm^{-1}. An estimation of tumor washout during SPECT acquisition was obtained by analyzing tumor regions of interest (ROIs) on the first and last SPECT image.

The reported radiation burden of IMT is 0.007 mSv/MBq, yielding an effective dose equivalent of 2.5–3.5 mSv (*32*).

Analysis of Metabolism

At 0, 10, 20, 30 min, 1, 3 and 24 hr postinjection, heparinized blood samples were collected from the first 10 patients. After centrifugation (3000 × g for 10 min), plasma samples were analyzed for total and trichloroacetic acid (TCA)-precipitable radioactivity using a gamma counter (Compugamma, LKB Wallac, Finland), together with a defined 1% aliquot of the injected material as reference. The measured radioactivity was expressed as a percentage of the injected dose (%ID) per liter of plasma. In addition, relative fractions of the parent compound IMT, ^{123}I and possible other metabolites were determined by elution of plasma samples over a C18 Sep-Pak cartridge, preconditioned with methanol followed by physiologic saline containing 5% ethanol. In two patients, 3- and 24-hr urine portions were collected and analyzed for total radioactivity and metabolites in the same manner as the plasma samples.

Data Analysis

Without knowledge of the clinical and histopathologic data, all images were analyzed visually for tumor uptake and abnormal extratumoral uptake. Normal uptake patterns were assessed visually from whole-body scans and from spot views. ROIs were placed manually over areas of abnormal uptake on 10-min summed initial dynamic images, on the SPECT slices with maximal lesion visibility and/or on spot views. ROIs were drawn at 80% of the maximal pixel value around the lesion under study (*33*). A representative, usually contralateral background region was defined, and ROI-size normalized tumor-to-background (T/B) ratios were calculated. To relate tumor-to-normal organ uptake, tumor-to-blood-pool ratios and tumor-to-liver ratios were calculated using an ROI method. All IMT scintigraphic findings were finally compared to standard conventional images (CT, MRI, mammography and ultrasound) and histology.

RESULTS

Metabolism

IMT was rapidly cleared from the plasma: 10 min after injection, only 3.6% ± 0.6% (mean ± s.d.) of total radioactivity was present per liter of plasma. Therefore, ~90% of the tracer had left the plasma compartment within the first 10 min (Fig. 1). The shape of the plasma disappearance curve was biphasic. Minor deiodination took place, starting from 7.5% (of plasma radioactivity, 10 min after injection) and rising to 24.5% free

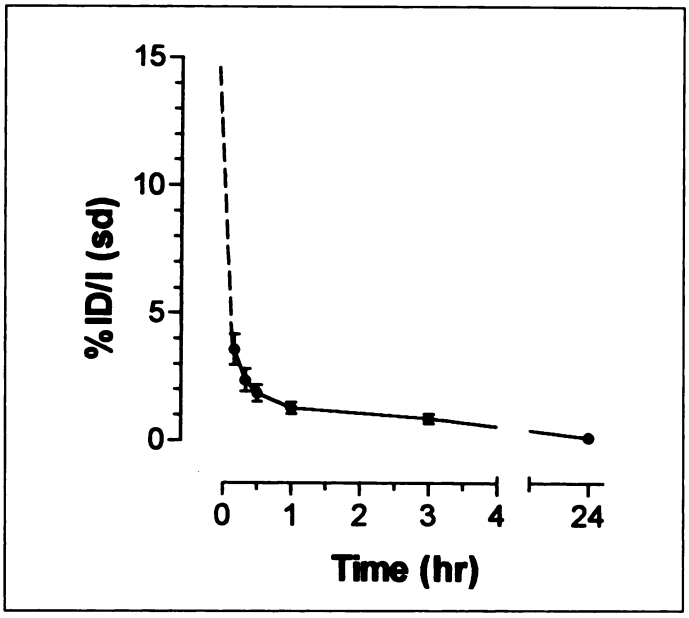

FIGURE 1. Plasma clearance of IMT. Total radioactivity (%ID per liters of plasma) with s.d. (bars) versus time (hr).

^{123}I 3 hr after injection (Table 2). This amounts to mean plasma iodide levels at 10 min, 1 hr and 3 hr of 0.8%ID (range 0.4%–1%), 0.7%ID (range 0.4%–0.9%) and 0.6%ID (range 0.4%–0.7%), respectively.

Renal excretion amounted to 40%–50% within the first 3 hr and to 65%–85% of the ID in 24 hr. In the urine excreted in the first 3 hr, 95% or total radioactivity consisted of intact IMT and the remaining 5% free iodide. In the 24-hr urine, 10%–15% free iodide was found; the remainder was intact IMT. Because intact IMT and free iodide together accounted for ~100% of the radioactivity both in plasma and in urine, it was concluded that no other labeled metabolites were formed.

A slowly decreasing fraction of plasma activity was TCA-precipitable, but IMT added to plasma in vitro also gave a TCA-precipitable fraction of 24% (Table 2). These data indicate coprecipitation of IMT with plasma proteins.

Neither immediate nor delayed side effects were observed after the administration of the radiopharmaceutical.

Normal Scintigraphic Appearance

The images indicate a high concentration in the kidneys and urinary tract. In the brain, diffuse uptake was noted in the first hour, which disappeared after 3 hr. Some uptake in the naso/oropharyngeal area, salivary glands, thyroid and stomach

TABLE 2
Analysis of Plasma Radioactivity After Administration of L-3-Iodine-Iodo-α-Methyl-Tyrosine

Time postinjection	% intact IMT	% free ^{123}I	% rest*	% TCA-precipitable†
10 min	89.8 ± 3.3	7.5 ± 2.8	2.3 ± 1.1	23.4 ± 4.5
20 min	86.3 ± 4.6	10.8 ± 4.7	2.2 ± 1.2	23.5 ± 4.6
30 min	83.5 ± 7.5	12.8 ± 4.9	3.2 ± 3.3	22.0 ± 4.4
1 hr	78.9 ± 8.0	18.0 ± 6.5	2.6 ± 2.2	20.5 ± 3.8
3 hr	73.0 ± 8.5	24.5 ± 7.9	2.1 ± 2.1	19.6 ± 5.0
24 hr	32.5 ± 3.1	61.6 ± 8.0	3.6 ± 1.4	15.8 ± 4.4

*Activity remaining on the C18 SepPak column.
†Control experiment: (after in vitro addition of IMT to plasma): 23.7% ± 5.8% TCA-precipitable.
Values represent mean ± s.d.; TCA = trichloroacetic acid.

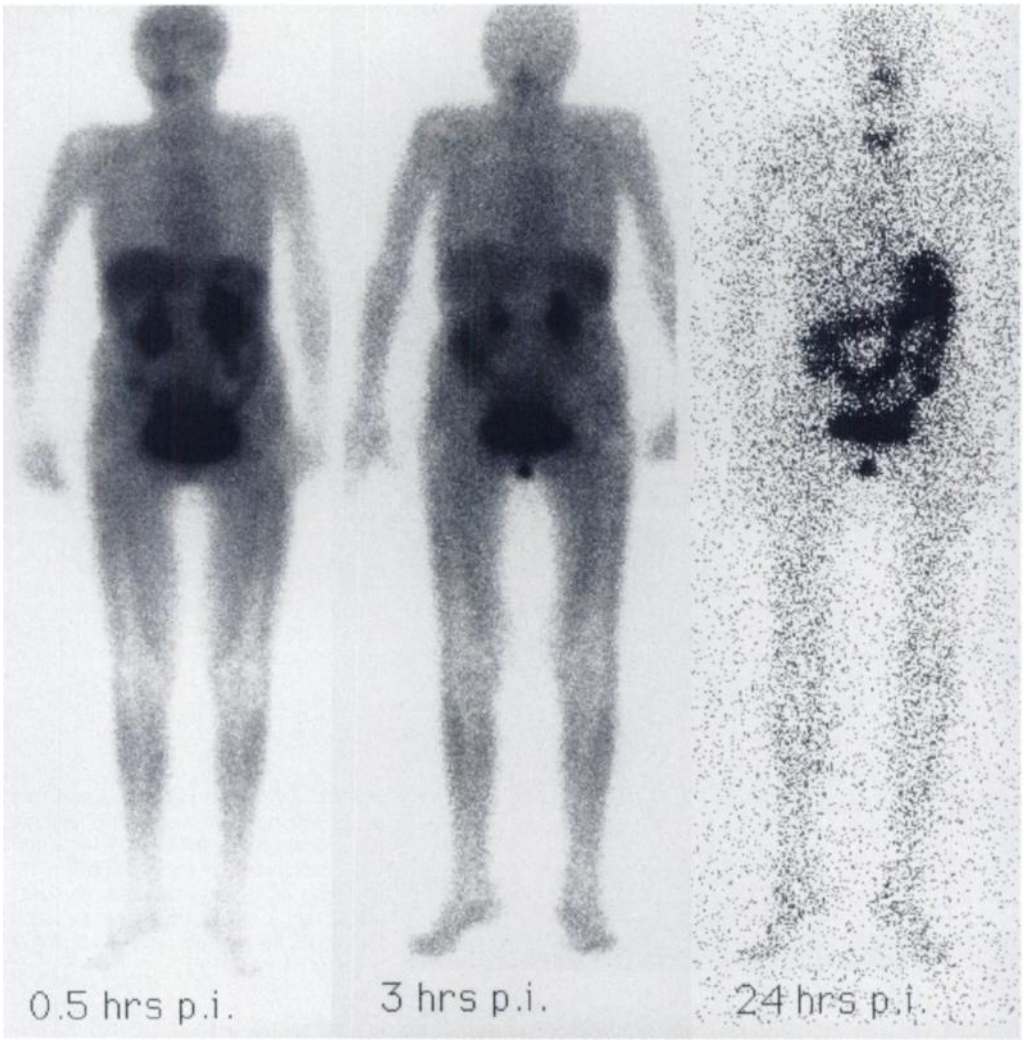

FIGURE 2. Whole-body scans acquired 0.5 hr (left), 3 hr (center) and 24 hr (right) postinjection of 350 MBq IMT.

was seen on the early scans, slightly increasing after 3 hr. No uptake was observed in the thoracic region, except for minor blood-pool and myocardial activity (n = 2) during the first 3 hr. Modestly intense uptake was present in the liver without the typical pattern of hepatobiliary clearance (no gallbladder or bile duct visualization). Some splenic uptake was observed. Accumulation in the pancreatic region, but intestinal structures were noted in the first hour after injection and were quite variable between patients and between the first and third hour in individual patients. Possible pancreatic uptake was present in 7 of 20 patients (35%) during the first hour only but was hard to separate from neighboring structures. In general, the 3-hr images showed slowly increasing bowel activity. In obese patients, it was clearly noted that uptake in muscles was higher than that in subcutaneous fat.

The scintiscans obtained 24 hr after administration showed uptake in the thyroid, naso/oropharynx and salivary glands and rather high uptake in the stomach and small intestinal structures. Most radioactivity (including tumor uptake) had disappeared by this time and, therefore, these 24-hr scintiscans were omitted after the first three patients. An example is shown in Figure 2.

Tumor Uptake

All malignant primary tumors were visualized. Examples are presented in Figures 3 and 4. Only the two metastatic carcinoid tumors in the liver were not visualized, one of which was very small. T/B ratios (Table 1) peaked within the first hour after administration and had decreased significantly in nearly all cases 3 hr postinjection (Fig. 5). During the ~30-min SPECT acquisition, tumor washout was estimated to be between 10% and 20% of the initial uptake, in the same range as neighboring normal tissues. After 24 hr, most radioactivity had disappeared, and no remaining tumor uptake was observed. When SPECT was performed (n = 16), this greatly improved the T/B ratio and lesion detectability.

In Patient 5, who had small-cell lung cancer, pathologic IMT uptake was observed in mediastinal and supraclavicular metastases (Fig. 4). In two cases of breast cancer, axillary metastases were present. In Patient 7, intense IMT uptake was noted in an axillary lymph node metastasis, whereas a microscopic metastasis was missed on the IMT SPECT scan of Patient 9. Another microscopic axillary lymph node metastasis could not be distinguished on planar IMT images of Patient 14. In two cases of bone metastases, as shown on a bone scintiscan, no IMT uptake could be assessed on planar images (Patients 8 and 10).

Patient 1 was imaged 2 wk after ileocecal resection of a large carcinoid tumor. During surgery, a 1-cm liver metastasis was suspected after liver palpation, but the biopsy showed only normal liver tissue. No abnormal IMT uptake was noted in the liver postoperatively. Patient 2 had a 5-cm carcinoid liver metastasis that showed no IMT uptake above the liver background. No SPECT was performed in this patient.

Compared with the nonbrain tumors, the IMT uptake in the two brain tumors (one low-grade mixed oligoastrocytoma and one high-grade glioma) was fairly low, with tumor uptake only slightly above the brain background.

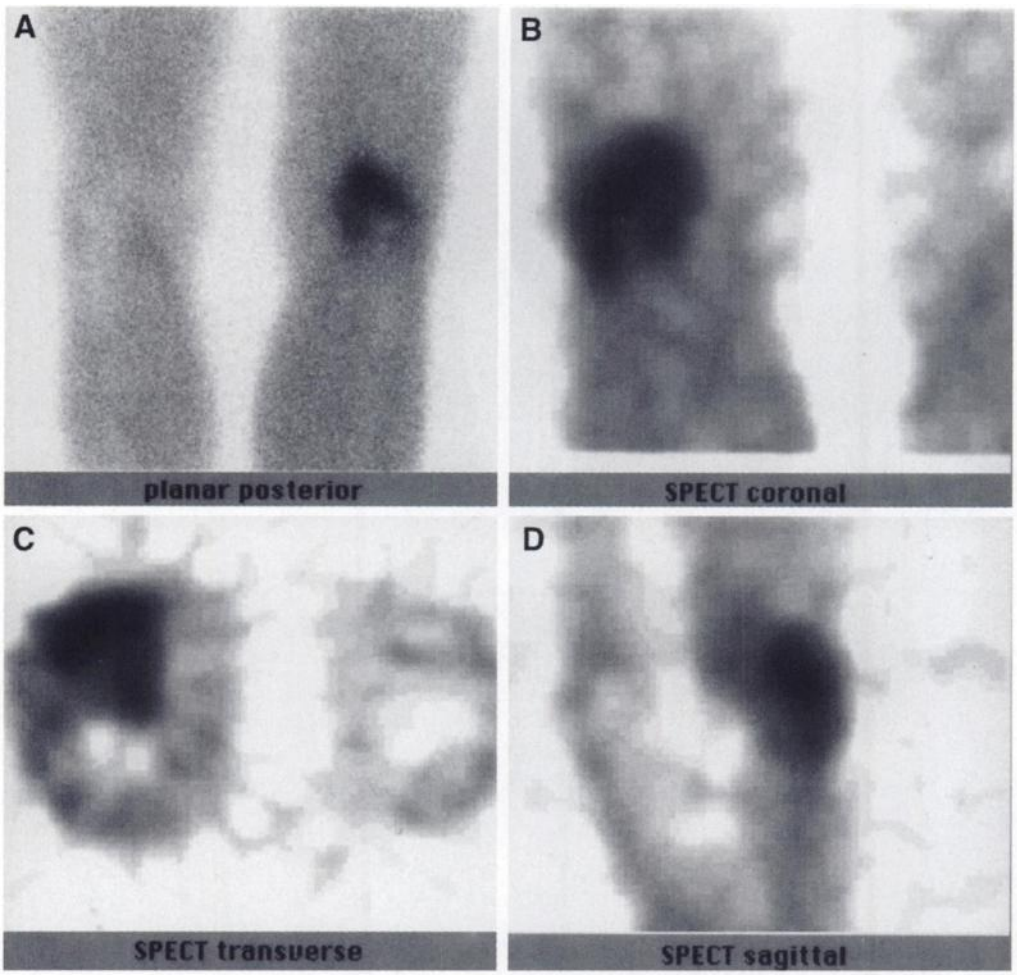

FIGURE 3. Posterior planar image 20 min postinjection (A) and sagittal (B), coronal (C) and transverse (D) SPECT slices (60 min postinjection) of knees in Patient 15, who had high-grade sarcoma dorsolateral to right distal femur showing intense tumor uptake after administration of 400 MBq IMT.

In two patients with breast cancer, imaging was repeated 6 wk after the termination of radiotherapy. In both cases, a marked decrease in uptake was present, in accordance with the clinical assessment (in Patient 4, complete disappearance; in Patient 8, partial disappearance of palpable lesions) (Fig. 6).

Uptake in Benign Processes

In Patient 13, very faint uptake, just above background and only detectable by SPECT, was observed in a large bony process dorsolateral to the right upper femur. MRI suggested this to be a osteoblastoma, on incisional biopsy, however, a nonspecific cortical thickening was found with some inflammatory cells. In Patient 6, a 2-cm coin lesion in the right lung showed very faint IMT uptake (exclusively on SPECT) and proved to be a very active focal vasculitis after pathologic examination.

In Patient 1, minor IMT uptake was observed in the operation field in the lower right abdomen 2 wk after ileocecal resection of the large carcinoid gut tumor. In Patient 10, multiple pulmonary granulomata exhibited no IMT uptake. Also, another benign lesion, a fibrous nodular hyperplastic lesion in the liver of Patient 11, showed no IMT uptake.

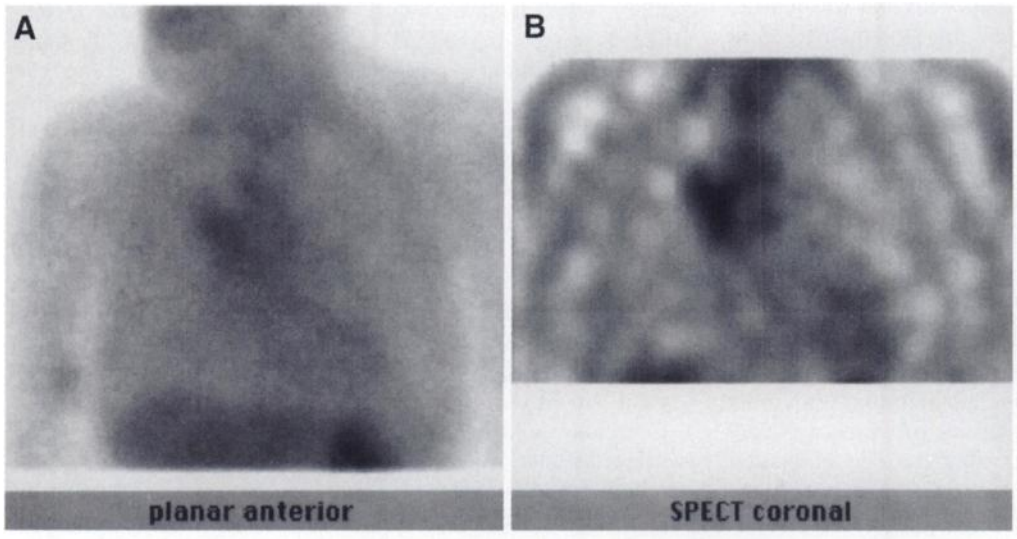

FIGURE 4. Anterior planar image (A) and coronal SPECT slice (B) of chest in Patient 5 showing intense uptake in primary tumor near right pulmonary hilus, lower and upper mediastinal lymph nodes and bilateral supraclavicular metastases. Images were obtained 20 min (planar) and 60 min (SPECT) after administration of 450 MBq IMT.

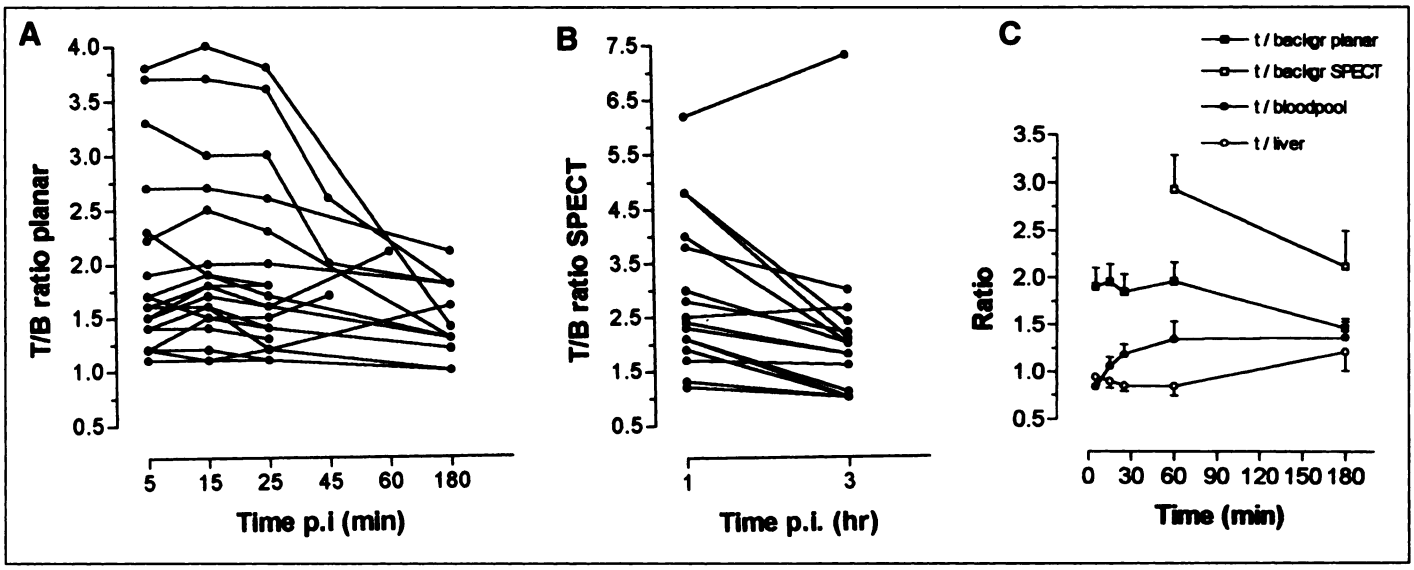

FIGURE 5. Tumor uptake, represented by the tumor-to-background (T/B) ratio over time, for all patients. (A) Data obtained from dynamic planar images and spot views. (B) Data obtained from early and delayed SPECT images (n = 16). (C) Average values (bars = s.d.) for T/B ratios, tumor-to-blood pool ratios and tumor-to-liver ratios versus time.

DISCUSSION

Although considerable experience exists in the imaging of brain tumors with the artificial amino acid IMT, no data are available regarding the use in other tumors. This study shows the feasibility of IMT and SPECT for the detection and therapy evaluation of extracranial tumors. We found good tumor uptake in breast tumors, lung tumors, malignant lymphomas and soft-tissue sarcomas.

T/B ratios in these nonbrain tumors were the same as or higher than those reported in primary brain tumors (*17,18,21,34*). Tumor uptake appeared to peak rapidly after administration, within the first 15–30 min, as was also observed in brain tumors (*18*). All tumors remained visible during the first hour, but after 3 hr, T/B ratios had considerably decreased in nearly all cases.

The uptake mechanism of IMT in brain tumors was studied by Langen et al. (*16*). They showed that IMT is not incorporated in protein, is not further metabolized and, after rapid uptake, slowly washes out of the brain. In addition, they demonstrated that brain and primary brain tumor uptake can be diminished by infusion of amino acids and, therefore, concluded that the uptake is mediated by amino acid transport, presumably by the large neutral amino acid carrier system in the blood–brain barrier (*16,17*). This competitive effect of amino acid loading on IMT uptake was much lower in one metastasis and two meningiomas. This finding suggests a different method of uptake in nonbrain tumors. However, the presence of the blood-brain barrier and the potential differences in the Michaelis–Menten constant for amino acid transport in brain tissue versus nonbrain tissue make the translation of observations in brain tumors to tumors elsewhere in the body very difficult (*35*).

The uptake mechanism of IMT in these tumors outside the brain is not known. However, some clues can be derived from our data and from the literature. The first clue is that IMT T/B ratios peak at ~30 min; at that time, total plasma activity has already decreased to ~6%ID (Fig. 1). Minor blood-pool activity can be caused by uptake into erythrocytes, a known phenomenon of amino acids. The second clue is that tumor-to-blood pool ratios rise during the first hour and then remain stable (Fig. 5C). Although nonspecific uptake by passive diffusion related to tumor blood flow could surely be present, these rising ratios may suggest (partial) specific uptake. The third clue is that, during the 30- to 40-min SPECT acquisition, normal tissue washout was not different from tumor washout (both 10%–20% of the initial value). The fourth clue is that the T/B ratios of many patients may be too high for just nonspecific uptake. Although we did not separately assess tumor blood flow, a limitation of this study, it is unlikely that tumor perfusion is, e.g., 4–6 times higher than perfusion in neighboring normal tissues.

Together, these clues may lead to the hypothesis that cellular tumor uptake is rapid and higher in malignant tissue than in normal tissue, whereas cellular washout of this artificial amino

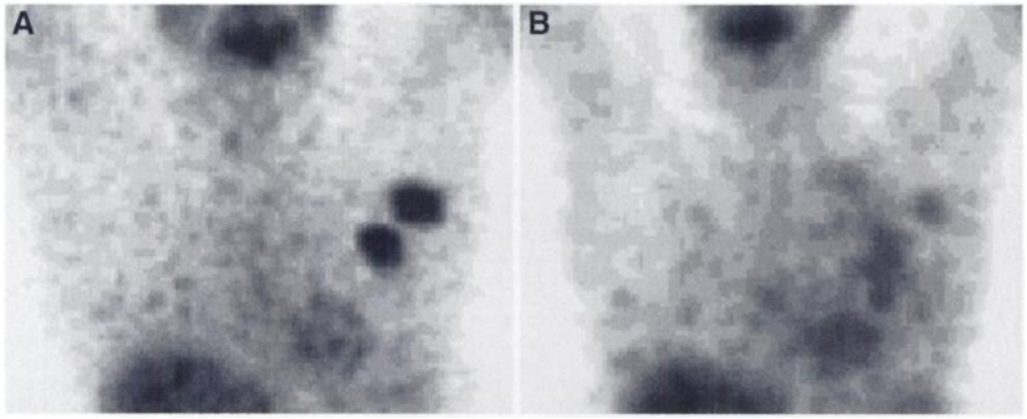

FIGURE 6. SPECT images (volume-rendered projections) of Patient 7 showing intense uptake in 3-cm left-sided breast carcinoma and in 3-cm axillary metastasis. Minor uptake in cardiac blood pool is observed. (A) Before radiotherapy. (B) Six weeks after termination of radiotherapy, a marked reduction in tumor uptake is noted. Images were obtained 1 hr after administration of 340 MBq IMT.

acid is the same for tumors and normal tissues. However, Deehan et al. (*27*) suggested that uptake of not only IMT, but also ^{11}C-labeled amino acids in artificial rat tumors, is related to blood flow and diffusion and, to a lesser extent, amino acid transport phenomena. On the other hand, they observed good tracer penetration in poorly vascularized areas. In contrast with their findings, other studies have demonstrated that (at least for ^{11}C-labeled amino acids) specific tumor uptake is present (*10*). In addition, all amino acids can enter cells by passive diffusion (*36*) Therefore, the exact uptake mechanism for IMT and the possible fraction of nonspecific uptake remain unclear. Although some influence of tumor perfusion is evident (and even necessary) for any tumor tracer, such as ^{201}Tl, ^{99m}Tc-sestamibi or FDG, this may not be clinically relevant as long as specific tumor uptake is also present. It is evident that more research is warranted in this area.

In addition to the tumor uptake analysis, normal whole-body patterns of IMT uptake were qualitatively established. IMT is rapidly cleared from the plasma (Fig. 1), but minor blood-pool activity and also myocardial uptake are noted on the images of a minority of our patients [also on the images provided by Schmidt et al. (*32*)]. This may be caused by amino acid transporter activity of erythrocytes and myocardial cells (*36*). Uptake in the brain is present during the first hour but has almost completely disappeared at 3 hr. Although IMT is a stable tracer (deiodination in plasma of 0.6%ID; range 0.4%–0.7%; 60 min postinjection), uptake in the thyroid, salivary glands, stomach and intestine was seen at 1 and 3 hr, and more uptake was seen at 24 hr. Langen et al. (*18*) found lower rates of deiodination in three patients. Uptake in the liver and spleen was present at 1 and 3 hr postinjection. Although biodistribution studies in mice have shown high uptake in the pancreas (*26*), we only observed possible pancreatic uptake in 35% of our patients, which was low and hard to distinguish from neighboring tissue uptake. In all patients, uptake in intestinal structures was present on the early images. The pattern of this was variable between patients and changing over time in individual patients. Intestinal uptake cannot be attributed to hepatobiliary clearance because gallbladder or bile duct visualization was absent in all dynamic studies in which the liver was in the field of view. These intestinal uptake patterns are also noted on PET amino acid studies and may be caused by amino acid uptake in metabolically active intestinal tissue. All patients were imaged after an overnight fast, but it is possible that intestinal and pancreatic uptake depends on dietary conditions of the preceding day. Our findings regarding the normal uptake and metabolic behavior of IMT are in close agreement with a recent publication by Schmidt et al. (*32*), who quantitatively described whole-body kinetics in six brain tumor patients.

The combination of intense renal and bladder activity, liver uptake and variable uptake in intestinal structures, stomach and pancreas makes abdominal pathology hard to investigate. Especially on SPECT filtered backprojection reconstructions, bladder/kidney artifacts are to be expected and, therefore, in this study we excluded patients with tumors in these areas. More experience is required, but bladder/kidney uptake may seriously limit clinical application in the abdominal area.

Although good uptake in various primary tumors and their metastases was present, microscopic disease in axilla and bone was below the detection limit, as this is the case for virtually every noninvasive and even invasive procedure. The isointense uptake in the patient with a 5-cm carcinoid liver metastasis may be attributed to a very low metabolic rate in this tumor that had been present for many years, but it probably also may be attributed to the omission of SPECT in this case. Although minor uptake in some inflammatory processes was observed, this could be distinguished from the more intense uptake in all other malignant tumors outside the brain (SPECT T/B ratio was >1.9 and planar T/B ratio was >1.2 in all cases) but not from the two brain tumors. Kuwert et al. (*21*) also found minor uptake in some nontumorous brain processes, limiting the differentiation between benign and low-grade malignant brain processes.

Some studies have suggested IMT SPECT to be of value in determining the response to radiotherapy of brain tumors, information that is hard to obtain by means of CT or MRI investigations (*6,24*). The correspondence between the IMT uptake and the clinical response after radiotherapy in the two patients with breast cancer in our study may lead to the speculation that IMT SPECT can provide useful clinical information on treatment evaluation in tumors outside the brain as well. Further work is warranted in this field.

Although our patient group is rather small and only contains a few tumor types, general tumor uptake of IMT appears to be of the same magnitude as uptake of ^{201}Tl, ^{99m}Tc-MIBI or ^{67}Ga. The extent of uptake appears not different from uptake in brain tumors. Also, uptake kinetics in peripheral tumors are similar to brain tumor kinetics. Because uptake in brain tumors reflects transport of amino acids, it is tempting to suggest that some part of the uptake in extracranial tumors is associated with amino acid transport. Addition of a general amino acid SPECT tracer might be a valuable addition to diagnosis and therapy evaluation, although interfering normal abdominal uptake and not completely neglectable free iodide production may limit whole-body analysis. Furthermore, it remains to be demonstrated whether IMT uptake is, indeed, a measure for amino acid transport activity in vivo.

As in brain tumors, the optimal scan protocol requires imaging within the first ~60–90 min after administration because that is when T/B ratios are highest. SPECT is recommended. The procedure proved to be a simple, patient-friendly, 1-day investigation with a reportedly low radiation burden. Further work in carefully selected patient groups is necessary to validate this method for tumor detection, staging and restaging, as well as further elucidating the uptake mechanism in nonbrain tumors.

CONCLUSION

We have shown that tumors outside the brain can be visualized using the labeled amino acid IMT.

ACKNOWLEDGMENTS

We thank J. Boorsma, C. Harms and A.K. van Zanten for developing and performing the radiosynthesis and the laboratory work.

REFERENCES

1. Lamki LM. Tissue characterization in nuclear oncology: its time has come. *J Nucl Med* 1995;36:207–210.
2. Conti PS, Lilien DL, Hawley K, Keppler J, Grafton ST, Bading JR. PET and [^{18}F]-FDG in oncology: a clinical update. *Nucl Med Biol* 1996;23:717–735.
3. Kubota K, Yamada K, Fukuda H, et al. Tumor detection with carbon-11-labeled amino acids. *Eur J Nucl Med* 1984;9:136–140.
4. Kubota K, Kubota R, Yamada S. Fluorodeoxyglucose accumulation in tumor tissue. *J Nucl Med* 1993;34:419–421.
5. Minn H, Joensuu, Ahonen A, et al. Fluorodeoxyglucose imaging: a method to assess the proliferative activity of human cancer in vivo. Comparison with DNA flow cytometry in head and neck tumors. *Cancer* 1988;61:1776–1781.
6. Di Chiro G, Oldfield E, Wright DC, et al. Cerebral necrosis after radiotherapy and/or intraarterial chemotherapy for brain tumors: PET and neuropathologic studies. *Am J Roentgenol* 1988;150:189–197.
7. Kubota K, Yamada S, Kubota R, Ishiwata K, Tamahashi N, Ido T. Intramural distribution of fluorine-18-fluorodeoxyglucose in vivo: high accumulation in macrophages and granulation tissues studied by microautoradiography. *J Nucl Med* 1992; 33:1972–1980.

8. Strauss LG. Fluorine-18-deoxyglucose and false-positive results: a major problem in the diagnostics of oncological patients. *Eur J Nucl Med* 1996;23:1409–1415.
9. Vaalburg W, Coenen HH, Crouzel C, et al. Amino acids for the measurement of protein synthesis in vivo by PET. *Nucl Med Biol* 1992;19:227–237.
10. Willemsen ATM, van Waarde, A, Paans AMJ, et al. In vivo protein synthesis rate determination with L-[1-C-11]tyrosine and PET: methods, metabolism, modeling and results in patients with primary or recurrent brain tumors. *J Nucl Med* 1995;36:411–419.
11. Kubota K, Ishiwata K, Kubota K, et al. Feasibility of fluorine-18-fluorphenylalanine for tumor imaging compared with carbon-11-L-methionine. *J Nucl Med* 1996;37:320–325.
12. Isselbacher KJ. Sugar and amino acid transport by cells in culture: differences between normal and malignant cells. *N Engl J Med* 1972;286:929–933.
13. Kubota K, Matsuzawa T, Fujiwara T, et al. Differential diagnosis of AH109A tumor and inflammation by radioscintigraphy with L-[methyl-^{11}C]-methionine. *Jpn J Cancer Res* 1989;80:778–782.
14. Kubota R, Kubota K, Yamada S, et al. Methionine uptake by tumor tissue: a microautoradiographic comparison with fluorodeoxyglucose. *J Nucl Med* 1995;36:484–492.
15. Martin WH, Delbeke D, Patton JA, Sandler MP. Detection of malignancies with SPECT versus PET, using 2-[fluorine-18]-fluoro-2-deoxy-D-glucose. *Radiology* 1996;198:225–231.
16. Langen KJ, Roosen N, Coenen HH, et al. Brain and brain tumor uptake of L-3-[^{123}I]Iodo-alpha-methyl-tyrosine: competition with natural L-amino acids. *J Nucl Med* 1991;32:1225–1228.
17. Oldendorf WH. Saturation of amino acid uptake by human brain tumor demonstrated by SPECT. *J Nucl Med* 1991;32:1229–1230.
18. Langen KJ, Coenen HH, Roosen N, et al. SPECT studies of brain tumors with L-3-[^{123}I]Iodo-alpha-methyl-tyrosine: comparison with PET, [^{124}I]IMT and first clinical results. *J Nucl Med* 1990;31:281–286.
19. Biersack HJ, Coenen HH, Stöcklin G, et al. Imaging of brain tumors with L-3-[^{123}I]Iodo-alpha-methyl-tyrosine and SPECT. *J Nucl Med* 1989;30:110–112.
20. Langen KJ, Ziemons K, Kiwit JCW, et al. 3-[^{123}I]Iodo-alpha-methyl-tyrosine and [methyl-^{11}C]-L-methionine uptake in cerebral gliomas: a comparative study using SPECT and PET. *J Nucl Med* 1997;38:517–522.
21. Kuwert T, Morgenroth C, Woesler B, et al. Uptake of iodine-123-alpha-methyl-tyrosine by gliomas and non-neoplastic brain lesions. *Eur J Nucl Med* 1996;23:1345–1353.
22. Otto L, Dannenberg C, Feyer P, et al. Brain tumors: effect of radiation therapy on amino acid transport [Abstract]. *Eur J Nucl Med* 1996;23(suppl):S3.
23. Wunderlich G, Schmidt D, Langen KJ, et al. Evaluation of chemotherapy in gliomas by ^{123}I-alpha-methyl-tyrosine SPECT. *Eur J Nucl Med* 1995;22:796.
24. Guth-Tougelides B, Müller S, Mehdorn MM, Knust EJ, Dutschka K, Reiners C. Uptake of DL-3-123I-iodo-alpha-methyl-tyrosine in recurrent brain tumors. *Nuklearmedizin* 1995;34:71–75.
25. Kloss G, Leven M. Accumulation of radioiodinated tyrosine derivatives in the adrenal medulla and in melanomas. *Eur J Nucl Med* 1979;4:179–186.
26. Tisljar U, Kloster G, Ritzal, Stöcklin G. Accumulation of radioiodinated L-alpha-methyl-tyrosine in pancreas of mice: concise communication. *J Nucl Med* 1979;20:973–976.
27. Deehan B, Carnochan P, Trivedi M, Tombs A. Uptake and distribution of L-3-[^{123}I]Iodo-alpha-methyl-tyrosine in experimental rat tumours: comparison with blood flow and growth rate. *Eur J Nucl Med* 1993;20:101–106.
28. Pruim J, Willemsen ATM, Paans AMJ, et al. Protein synthesis rate (PSR) measured with L-[1-C-11]tyrosine in soft tissue tumors (STT) [Abstract]. *J Nucl Med* 1995;36:217P.
29. Kole AC, Nieweg OE, Pruim J, et al. L-1-[^{11}C]-tyrosine, a better tracer for breast cancer visualization and quantification of metabolism [Abstract]. *J Nucl Med* 1996;37:86P.
30. Kole AC, Pruim J, Nieweg OE, et al. PET with L-[1-carbon-11]-tyrosine to visualize tumors and measure protein synthesis rates. *J Nucl Med* 1997;38:191–195.
31. Krummeich C, Holschback M, Stöcklin G. Direct n.c.a. electrophilic radioiodination of tyrosine analogues: their in vivo stability and brain-uptake in mice. *Appl Radiat Isot* 1994;45:929–935.
32. Schmidt D, Langen KJ, Herzog H, et al. Whole-body kinetics and dosimetry of L-3-[^{123}I]iodo-alpha-methyl-tyrosine. *Eur J Nucl Med* 1997;24:1162–1166.
33. Kuwert T, Morgenroth C, Woesler B, et al. Influence of size of regions of interest on the measurement of uptake of ^{123}I-alpha-methyl-tyrosine by brain tumors. *Nucl Med Commun* 1996;17:609–615.
34. Weber W, Bartenstein P, Gross M, et al. Fluorine-18-FDG PET and Iodine-123-IMT SPECT in the evaluation of brain tumors. *J Nucl Med* 1997;38:802–808.
35. Partridge WM, Oldendorf WH, Cancilla P, et al. Blood–brain barrier: interface between internal medicine and the brain. *Ann Intern Med* 1986;105:82–95.
36. Souba WW, Pacitti AJ. How amino acids get into cells: mechanisms, models, menus, and mediators. *J Parent Ent Nutr* 1992;16:569–578.

Iodine-131-MIBG Therapy of a Patient with Carcinoid Liver Metastases

Elizabeth M. Prvulovich, Robert C. Stein, Jamshed B. Bomanji, Jonathon A. Ledermann, Irving Taylor and Peter J. Ell
Institute of Nuclear Medicine, Meyerstein Institute of Oncology, and Department of Surgery, University College London Medical School, London, United Kingdom

Iodine-131-metaiodobenzylguanidine (MIBG) is highly concentrated by >60% of carcinoid metastases and thus provides a therapeutic oppportunity. **Methods:** A symptomatic patient with carcinoid liver metastases, unresponsive to chemotherapy combined with interferon-alpha, was subsequently treated with ^{131}I-MIBG. **Results:** Radionuclide therapy, which was without significant side effects, resulted in symptomatic improvement and reduced urinary 5-hydroxyindoleacetic acid levels. No new metastases were observed for 15 mo after ^{131}I-MIBG therapy. Gross cystic change occurred in existing liver metastases, presumably as a result of ischemic necrosis. Surgical deroofing and aspiration of cysts led to regeneration of normal liver tissue. **Conclusion:** Iodine-131-MIBG therapy can provide prolonged symptomatic relief and improved quality of life in patients with metastatic carcinoid disease unresponsive to other therapies. The antitumor effect of ^{131}I-MIBG was accompanied by few side effects, suggesting that this therapy should be considered in symptomatic patients with an early stage of disease.

Key Words: iodine-131-metaiodobenzylguanidine; liver carcinoid; pseudocyst

J Nucl Med 1998; 39;1743–1745

Received Oct. 24, 1997; revision accepted Jan. 12, 1998.
For correspondence or reprints contact: Jamshed B. Bomanji, MD, Institute of Nuclear Medicine, Middlesex Hospital, Mortimer St., London W1N 8AA, United Kingdom.

Carcinoid liver metastases are common but are only rarely amenable to resection. Medical therapy aims to control symptoms and to extend survival by affecting tumor growth. Therapeutic options for symptomatic patients with unresectable disease include chemotherapy, interferon-alpha and octreotide (a somatostatin analog), but response to these treatments is often poor. Hepatic artery ligation or embolization are alternative options and have a better response rate. External beam radiotherapy has been tried in a small number of patients, and a good palliative response has been reported. Iodine-131-metaiodobenzylguanidine (MIBG), a guanethidine analog, is highly concentrated by >60% of carcinoid metastases (*1*) and thus provides an alternative therapeutic opportunity.

CASE REPORT

A 55-yr-old woman presented in November 1993 with a 6-mo history of flushing, diarrhea, abdominal pain and weight loss. Clinical examination was unremarkable. Urinary 5-hydroxyindoleacetic acid (5HIAA) levels were elevated at 596 μmol/24 hr (normal range < 45μmol/24 hr). CT revealed several space-occupying lesions in the liver (Fig. 1A); liver function tests were normal. Liver biopsy revealed monotonous tumor cells staining positive for chromogranin A, indicating metastatic carcinoid tu-